Small molecule modulation of Smoothened activity

James K. Chen, Jussi Taipale, Keith E. Young, Tapan Maiti, and Philip A. Beachy*

Department of Molecular Biology and Genetics, Howard Hughes Medical Institute, Johns Hopkins University School of Medicine, Baltimore, MD 21205

Smoothened (Smo), a distant relative of G protein-coupled receptors, mediates Hedgehog (Hh) signaling during embryonic development and can initiate or transmit ligand-independent pathway activation in tumorigenesis. Although the cellular mechanisms that regulate Smo function remain unclear, the direct inhibition of Smo by cyclopamine, a plant-derived steroidal alkaloid, suggests that endogenous small molecules may be involved. Here we demonstrate that SAG, a chlorobenzothiophene-containing Hh pathway agonist, binds to the Smo heptahelical bundle in a manner that antagonizes cyclopamine action. In addition, we have identified four small molecules that directly inhibit Smo activity but are structurally distinct from cyclopamine. Functional and biochemical studies of these compounds provide evidence for the small molecule modulation of Smo through multiple mechanisms and yield insights into the physiological regulation of Smo activity. The mechanistic differences between the Smo antagonists may be useful in the therapeutic manipulation of Hh signaling.

Hedgehog (Hh) signaling normally functions to specify embryonic pattern by directing cellular differentiation and proliferation (1), whereas aberrant Hh pathway activation is associated with the formation of tumors such as basal cell carcinoma and medulloblastoma (2–4). Cellular responses to the secreted Hh polypeptide are mediated by two integral membrane proteins, Patched (Ptc) and Smoothened (Smo), which were first identified by genetic screens in *Drosophila* (5–9). Hh binds to the twelve-pass transmembrane protein Ptc (8, 10, 11), thereby alleviating Ptc-mediated suppression of Smo (12), a distant relative of G protein coupled receptors. Smo activation then triggers a series of intracellular events, culminating in the stabilization of the transcription factor Cubitus interruptus (Ci) and the expression of Ci-dependent genes (13, 14). These events are recapitulated during mammalian development and tumorigenesis through multiple protein homologues, including three distinct Hh family members [Sonic (Shh), Indian (Ihh), and Desert (Dhh)], two Ptc proteins (Ptch1 and Ptch2), and three Ci-like transcription factors (Gli1, Gli2, and Gli3; ref. 1). In contrast, there is a single vertebrate homologue of Smo, which is implicated in all forms of Hh signaling by genetic analyses in *Drosophila*, mice, and zebrafish (15–18).

Despite this central role of Smo as mediator of all Hh signaling, the mechanisms by which Smo activation is regulated and coupled to downstream components remain enigmatic. Studies in *Drosophila* have shown that Hh stimulation is associated with changes in the phosphorylation state and subcellular localization of Smo (19, 20), but the relationship of these events to Smo activation is not known. How Ptc inhibits Smo function is also not well understood, although it appears that Ptc acts catalytically (21). It is similarly unclear how structural perturbations such as those found in an oncogenic Smo mutant (W539L; SmoA1) cause constitutive pathway activation. Recent studies in our laboratory suggest that Smo regulation may involve endogenous small molecules. The plant-derived steroidal alkaloid, cyclopamine, antagonizes Hh signaling (22–24) by binding directly to the Smo heptahelical domain (25), and Ptc is structurally related to the resistance-nodulation-cell division (RND) family of prokaryotic permeases and to the Niemann-Pick C1 (NPC1) protein, both of which are capable of transporting hydrophobic compounds (26, 27). Thus, Ptc might control Smo function by influencing its interactions with cellular small molecules.

To study the biochemical basis of Smo activation further, we set out to identify and characterize other small molecules that modulate Smo function. We report here that a family of chlorobenzothiophene molecules identified as Hh pathway agonists (28) act by binding to the Smo heptahelical bundle. We also describe four previously uncharacterized Smo antagonists discovered through small molecule screens for Hh pathway inhibitors. In addition to providing mechanistic insights, such modulators may have therapeutic potential, as demonstrated by the beneficial effects of cyclopamine in treating a mouse model of medulloblastoma (29).

Materials and Methods

Preparation of Synthetic Compounds. Procedures for the chemical synthesis of compounds described in this report are included in *Supporting Text*, which is published as supporting information on the PNAS web site, www.pnas.org.

Cell-Based Assays for Hh Pathway Activation. Assays for Hh pathway activation in Shh-LIGHT2 cells, a clonal NIH 3T3 cell line stably incorporating Gli-dependent firefly luciferase and constitutive *Renilla* luciferase reporters, were conducted as described (24). For studies of SAG (a chlorobenzothiophene-containing Hh pathway agonist) and PA-SAG, Shh-LIGHT2 cells were cultured to confluency in 96-well plates and then treated with various concentrations of these compounds in DMEM containing 0.5% (vol/vol) bovine calf serum.

SmoA1-LIGHT2 cells are a clonal NIH 3T3 cell line stably incorporating a Gli-dependent firefly luciferase reporter, a constitutive [thymidine kinase promoter] β-galactosidase reporter, and a constitutive [cytomegalovirus promoter] SmoA1 expression construct (24). These cells were cultured to confluency in 96-well plates using DMEM containing 10% (vol/vol) bovine calf serum, zeocin, and G418 and then treated with various concentrations of the indicated compounds in DMEM containing 0.5% bovine calf serum. After incubation at 37°C for 30 h, cellular firefly luciferase and β-galactosidase activities were measured by using chemiluminescence.

Assays for Hh pathway activation in P2$^{Ptch1-/-}$ cells, fibroblasts derived from mouse embryos lacking Ptch1 function, were conducted as described (24).

To study the effects of Ptch1 expression levels on SAG activity, NIH 3T3 cells were cultured in 96-well plates and transfected with the Gli-dependent firefly luciferase and simian virus 40 promoter containing *Renilla* luciferase reporters (50 ng per well; 20:1 plasmid ratio) and varying amounts of a mouse Ptch1 expression construct (0, 1, 5, and 25 ng per well). An expression construct for GFP was used to normalize total transfected DNA levels. Two days after transfection, the confluent NIH 3T3 cells were treated with varying concentrations of SAG (0–1.5 μM) in DMEM containing 0.5% (vol/vol) bovine calf serum for 30 h at 37°C. Cellular firefly and *Renilla* luciferase activities were then measured (24).

BIOCHEMISTRY

Preparation of Smo Fusion Proteins and Deletion Mutants. Smo-Myc$_3$ and SmoA1-Myc$_3$ contain three consecutive Myc epitopes at the protein C terminus. The deletion mutant SmoΔCRD lacks amino acids 68–182, and SmoΔCT lacks amino acids 556–793. All constructs were generated by PCR and verified by DNA sequencing.

Photoaffinity Labeling of Smo Proteins. Cross-linking studies of Smo-Myc$_3$ with PA-cyclopamine were conducted as described (25). Analogous procedures were used for PA-SAG: each well of transfected Cos-1 cells was incubated with ^{125}I-labeled PA-SAG [1 μCi (1 Ci = 37 GBq); ≈0.5 nM final concentration] and the indicated compounds, and Cos-1 cells expressing GFP were used as a control.

Fluorescence Binding Assays. Fluorescence binding assays using BODIPY-cyclopamine were conducted as described (25). For binding assays using fixed cells, Cos-1 cells were transfected in 15-cm dishes with a Smo expression vector, trypsinized, and fixed with 4% (wt/vol) paraformaldehyde for 10 min at room temperature. The cells were washed, resuspended in phenol red-free DMEM containing 0.5% (vol/vol) bovine calf serum, and incubated with 5 nM BODIPY-cyclopamine and the indicated competitors for 1 h at room temperature. The treated cells then were collected by centrifugation and analyzed by flow cytometry.

Small Molecule Screens for Hh Pathway Modulators. Compounds (10,000) were acquired from Chembridge (San Diego) as DMSO solutions in 96-well format. Shh-N (N-terminal fragment of Shh without cholesterol modification)-conditioned medium was obtained from an HEK 293 cell line stably transfected with Shh-N expression and neomycin resistance constructs. The Shh-N-producing HEK 293 cells were grown to 80% confluency in DMEM containing 10% (vol/vol) FBS and 400 μg/ml G418. The medium then was replaced with DMEM containing 2% (vol/vol) FBS, and after 1 day of growth, the medium was collected and filtered through a 0.22-μm membrane. Control medium was obtained from HEK 293 cells. Shh-LIGHT2 cells were then cultured to confluency in 96-well plates and treated with the small molecules (0.714 μg/ml; ≈2 μM compound in each well) in the presence of either Shh-N-conditioned medium or HEK 293 control medium (1:25 dilution into DMEM containing 0.5% bovine calf serum). After incubating the treated cells for 30 h at 37°C, cellular firefly and *Renilla* luciferase activities were measured (24).

Results

SAG, a Synthetic Hh Pathway Agonist, Regulates Smo Activity. Synthetic compounds with Hh pathway-modulating activity have recently been described (28), including a family of chlorobenzothiophene molecules capable of activating signal transduction in an Hh protein-independent manner (28). To investigate the molecular mechanism by which these molecules act, we began by demonstrating that one of these compounds, here named SAG (Fig. 1*A*), induces pathway activation in a mouse cultured cell assay (Shh-LIGHT2; ref. 24) with an EC$_{50}$ of ≈3 nM (Fig. 1*B*). Although the potency of this small molecule in pathway activation is similar to that of the processed N-terminal fragment of Shh (ShhNp), it differs in that pathway activity decreases dramatically as SAG concentration surpasses 1 μM (discussed more fully below).

Consistent with this differential activity profile, SAG is distinct from ShhNp in its mode of action. Whereas ShhNp induces pathway activation by inhibiting Ptch1 and/or Ptch2 function, SAG activity is independent of the Ptch proteins, as demonstrated by its effect on P2$^{Ptch1-/-}$ cells (24, 30). Treatment of these cells with 100 nM KAAD-cyclopamine, a potent cyclopamine derivative (IC$_{50}$ = 20 nM in the Shh-LIGHT assay; ref.
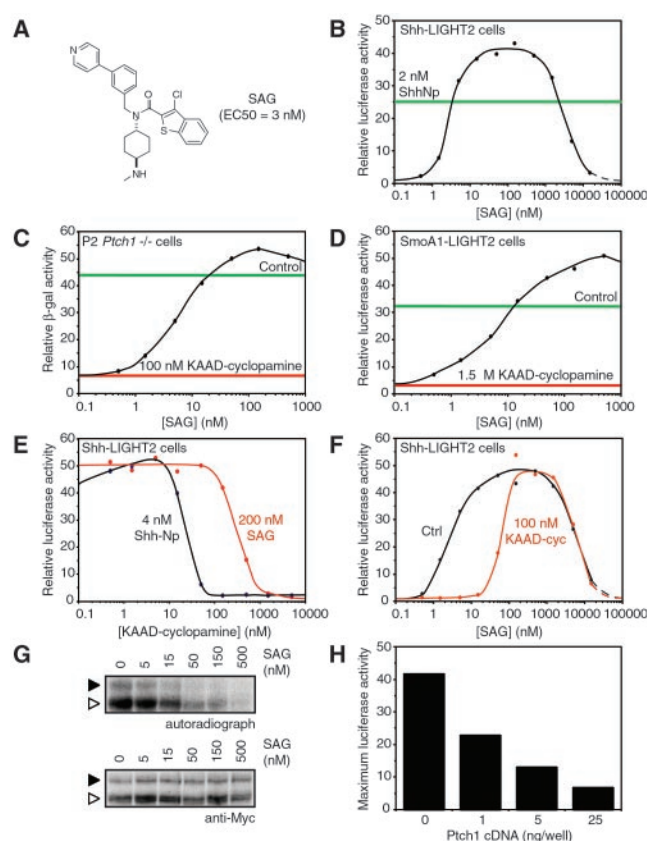
Fig. 1. SAG acts downstream of Ptch1 in the Hh pathway and counteracts cyclopamine inhibition of Smo. (*A*) Chemical structure of SAG and its activity in Shh-LIGHT2 cells. (*B*) SAG induces firefly luciferase expression in Shh-LIGHT2 cells with an EC$_{50}$ of 3 nM and then inhibits expression at higher concentrations. For comparison, the luciferase activity induced by 2 nM ShhNp is indicated by the green line. (*C*) SAG induces β-galactosidase expression in P2$^{Ptch1-/-}$ cells treated with 100 nM KAAD-cyclopamine. Hh pathway activation in these cells is indicated by β-galactosidase activity, because expression of this reporter enzyme is under the control of the *Ptch1* promoter, and *Ptch1* itself is a transcriptional target of Hh signaling. Observed β-galactosidase activities in the absence of pharmacological modulation and with 100 nM KAAD-cyclopamine alone are indicated by the green and red lines, respectively. (*D*) SAG induces firefly luciferase expression in SmoA1-LIGHT2 cells treated with 1.5 μM KAAD-cyclopamine. Luciferase activities in the absence of small molecules and in the presence of 1.5 μM KAAD-cyclopamine alone are depicted by the green and red lines, respectively. (*E*) Cyclopamine and SAG have antagonistic effects on Hh pathway activation in Shh-LIGHT2 cells. Fifteenfold higher concentrations of KAAD-cyclopamine are required to inhibit luciferase expression induced by 100 nM SAG (red trace) than are necessary to block luciferase expression induced by 4 nM ShhNp (black trace). Relative luciferase activities are normalized with respect to maximum activity levels. (*F*) Similarly, 20 times more SAG is required to activate the Hh pathway in cells treated with 200 nM KAAD-cyclopamine (red trace) than is necessary to activate the pathway to comparable levels in untreated Shh-LIGHT2 cells (black trace). (*G*) Cross-linking of ER-localized (white arrowhead; see text and ref. 25) and post-ER (black arrowhead) forms of Smo-Myc$_3$ in Cos-1 cells with ^{125}I-labeled PA-cyclopamine is inhibited by SAG in a dose-dependent manner (*Top*). Cellular levels of Smo-Myc$_3$ are not affected by agonist treatment (*Bottom*). (*H*) Ptch1 inhibits SAG-induced pathway activation in a dose-dependent manner. NIH 3T3 cells were transiently transfected with the Gli-dependent firefly luciferase reporter and varying amounts of a Ptch1 expression construct. Transfected cells then were treated with a range of SAG concentrations, and the maximum luciferase activities observed for each amount of transfected Ptch1 cDNA are shown. All firefly luciferase and β-galactosidase activities are the average of three experiments and are normalized relative to a control reporter.

24), completely suppressed the constitutive pathway activation resulting from loss of Ptch1 function. This activity was restored by simultaneous addition of SAG (Fig. 1*C*), indicating that the

cellular target of SAG is downstream of Ptch1. SAG similarly overcame KAAD-cyclopamine-mediated pathway inhibition in SmoA1-overexpressing cells (SmoA1-LIGHT2 cells; Fig. 1D), which also exhibit constitutive pathway activation in the absence of exogenous small molecules. These observations indicate that SAG acts on the Hh pathway at the level of Smo or on a downstream component.

We mapped the site of SAG action further by evaluating its functional and biochemical interactions with cyclopamine. SAG and cyclopamine activities are mutually antagonistic, consistent with opposing actions on a common target. For example, inhibition of pathway activation induced by SAG required a 15-fold higher concentration of KAAD-cyclopamine than that observed in ShhNp-stimulated cells (Fig. 1E), and SAG activity in Shh-LIGHT2 cells was attenuated 20-fold by the addition of 200 nM KAAD-cyclopamine (Fig. 1F). Biochemical evidence for this antagonistic relationship was then obtained by demonstrating the ability of SAG to inhibit the cross-linking of Smo expressed in Cos-1 cells by an ^{125}I-labeled photoaffinity derivative of cyclopamine (PA-cyclopamine) (ref. 24; Fig. 1G). These results suggest that Smo is the target of SAG action within the Hh pathway, either through a direct interaction or an intermediate component. Accordingly, increased Ptch1 expression reduces the maximum levels of SAG-induced pathway activation in NIH 3T3 cells (Fig. 1H).

SAG Binds Directly to the Smo Heptahelical Bundle. To examine the possibility of direct action of SAG on Smo, we used a photoaffinity reagent, PA-SAG, that activates the Hh pathway in Shh-LIGHT2 cells, albeit with some attenuation in potency ($EC_{50} = 250$ nM; Fig. 2A). We then expressed Smo in Cos-1 cells to produce endoplasmic reticulum (ER)-localized and post-ER forms of Smo, as previously characterized by endo H digestion and subcellular localization studies (25). Photoactivation of ^{125}I-labeled PA-SAG in transfected Cos-1 cells labeled the post-ER form of Smo but not the ER-localized forms of Smo or SmoA1 (Fig. 2B). This result contrasts the ability of SAG itself to inhibit the cross-linking of both ER-localized and post-ER Smo by PA-cyclopamine (see Fig. 1G). In any case, PA-SAG labeling of post-ER Smo is because of specific binding, as SAG inhibited this reaction in a range comparable to that required to inhibit PA-cyclopamine/Smo cross-linking ($IC_{50} = 15–50$ nM; Fig. 2 C and G), and there was essentially no cross-linking to non-native, SDS-resistant Smo aggregates. Consistent with the mutual antagonism of SAG and cyclopamine activities, KAAD-cyclopamine also was able to inhibit PA-SAG/Smo cross-linking, although surprisingly this inhibition required concentrations of KAAD-cyclopamine ($IC_{50} \approx 500$ nM; Fig. 2D) significantly greater than those necessary for inhibiting PA-cyclopamine/Smo cross-linking ($IC_{50} = 15–50$ nM; ref. 25). These observations demonstrate that SAG activates the Hh pathway by binding directly to Smo. The affinity of SAG for Smo was then determined by evaluating its inhibitory activity toward the binding of a fluorescent cyclopamine derivative (BODIPY-cyclopamine; ref. 25) to Smo-expressing Cos-1 cells. SAG blocked this association in a dose-dependent manner, yielding an apparent dissociation constant (K_D) of 59 nM for the SAG/Smo complex (Fig. 2E).

Having established Smo as the direct cellular target of SAG, we next investigated the structural determinants of Smo required for SAG binding. We previously found that BODIPY-cyclopamine can also bind cells expressing Smo proteins that lack either the N-terminal, extracellular cysteine-rich domain (SmoΔCRD) or the cytoplasmic C-terminal domain (SmoΔCT; ref. 25). The binding of BODIPY-cyclopamine to the Smo-deletion mutants was inhibited by 150 nM SAG to an extent similar to that observed with cells expressing WT Smo (Fig. 2F), indicating that SAG binds to all three Smo proteins with
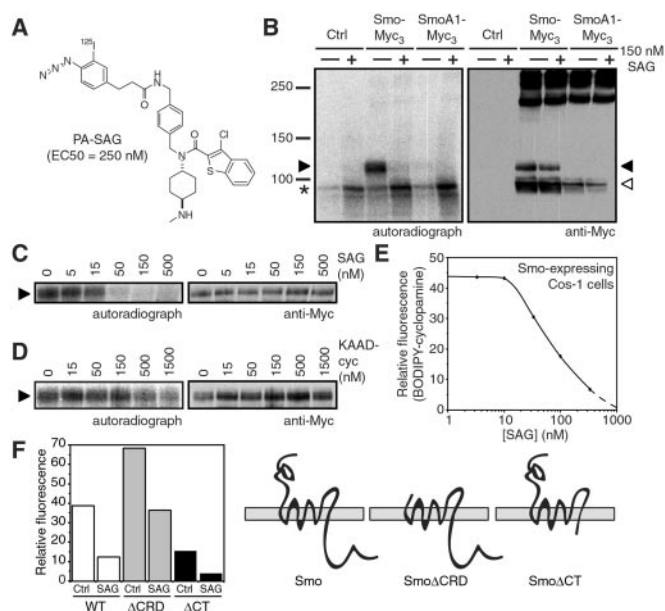

Fig. 2. SAG binds directly to Smo heptahelical bundle. (A) Chemical structure of the photoaffinity reagent PA-SAG and its activity in Shh-LIGHT2 cells. (B) ^{125}I-labeled PA-SAG cross-links the post-ER form of Smo-Myc$_3$ (black arrowhead) expressed in Cos-1 cells upon photoactivation, and this reaction is inhibited by 150 nM SAG (Left). The ER-localized form of Smo-Myc$_3$ (white arrowhead) is not detectably cross-linked, and cells expressing GFP as a control or SmoA1-Myc$_3$ do not yield specifically cross-linked products. An endogenous Cos-1 protein that is nonspecifically labeled by PA-SAG is denoted by the asterisk. Expression levels of Smo-Myc$_3$ and SmoA1-Myc$_3$ as determined by Western analysis are shown for comparison (Right). (C) SAG competes for PA-SAG cross-linking of post-ER Smo-Myc$_3$ (Left) in a manner similar to its ability to inhibit PA-cyclopamine cross-linking of Smo-Myc$_3$ (see Fig. 1G). Cellular levels of post-ER Smo-Myc$_3$ are not affected by SAG (Right). (D) KAAD-cyclopamine inhibits PA-SAG cross-linking of post-ER Smo-Myc$_3$, but concentrations greater than its apparent K_D for Smo (23 nM; ref. 25) are required (Left). Expression levels of post-ER Smo-Myc$_3$ are shown for comparison (Right). (E) SAG competes for the binding of BODIPY-cyclopamine to Smo-expressing cells, yielding an apparent dissociation constant of 59 nM for the SAG/Smo complex. (F) The binding of BODIPY-cyclopamine to Cos-1 cells expressing Smo, SmoΔCRD, or SmoΔCT is inhibited by 150 nM SAG with similar potencies, demonstrating that the SAG-binding site is localized to the Smo heptahelical bundle.

comparable affinities. As observed in our earlier studies, the different levels of BODIPY-cyclopamine binding associated with Smo, SmoΔCRD, and SmoΔCT likely reflect variations in protein expression levels (25). Thus, SAG interacts with the heptahelical bundle of Smo and does not require the cytoplasmic tail or CRD for binding.

Other Small Molecules Antagonize Smo Activity. Cyclopamine and SAG each bind the heptahelical bundle of Smo, yet these two compounds have opposing effects on Smo activity. To understand Smo regulation through small molecule binding better, we identified six additional effectors of the pathway using the Shh-LIGHT2 assay in a high-throughput format. Four of these compounds (SANT-1 through SANT-4; Fig. 3A) potently inhibit Shh signaling (Fig. 3B) by binding directly to Smo, as indicated by their ability to inhibit the association of BODIPY-cyclopamine with Smo-expressing cells (Fig. 3C). The other two Hh pathway inhibitors appear to act downstream of Smo (J.K.C. and P.A.B., unpublished data).

The four Smo antagonists display an interesting range of similarities and differences in comparison to cyclopamine and to each other (Table 1). Like cyclopamine (25), SANT-2, -3, and -4

BIOCHEMISTRY
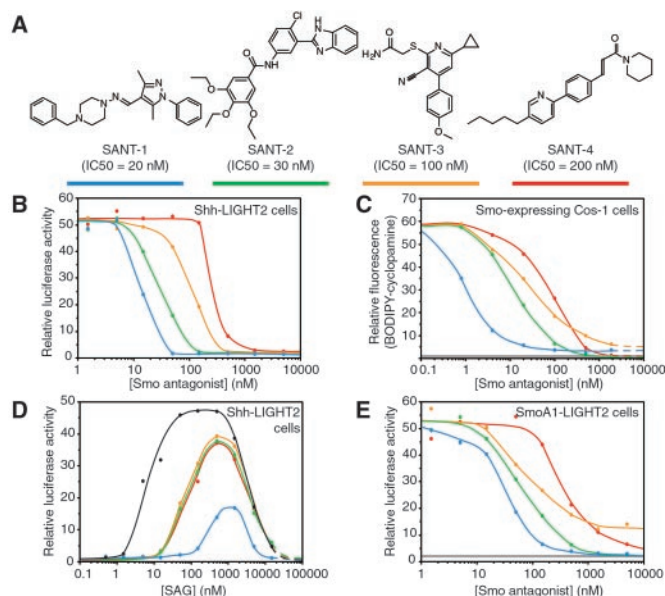
Fig. 3. Smo antagonists identified from a screen of 10,000 small molecules. (*A*) Chemical structures of SANTs and their activities in the Shh-LIGHT2 assay. The color-coding scheme used in the graphs is depicted by the blue, green, orange, and red lines. (*B*) The SANT compounds inhibit ShhNp-induced firefly luciferase expression in Shh-LIGHT2 cells. (*C*) The SANT molecules block the binding of BODIPY-cyclopamine to Smo-expressing Cos-1 cells, but SANT-1 and SANT-3 are unable to reduce BODIPY-cyclopamine binding to nonspecific levels. Nonspecific binding as defined by cellular BODIPY-cyclopamine levels in the presence of 500 nM KAAD-cyclopamine is indicated by the gray line. (*D*) Higher SAG concentrations are required to induce luciferase expression in Shh-LIGHT2 cells treated with 100 nM SANT-1 (blue trace), 150 nM SANT-2 (green trace), 500 nM SANT-3 (orange trace), or 1 μM SANT-4 (red trace) than are necessary to induce comparable luciferase activities in untreated Shh-LIGHT2 cells (black trace). (*E*) Unlike cyclopamine and its derivatives, the SANT compounds inhibit constitutive firefly luciferase expression in SmoA1-LIGHT2 cells with potencies that are similar to those required to inhibit Shh signaling in the Shh-LIGHT2 cells. Note that SANT-3 cannot completely inhibit luciferase expression in the SmoA1-LIGHT2 cells. Luciferase activity in SmoA1-LIGHT2 cells treated with 15 μM KAAD-cyclopamine is indicated by the gray line. All firefly luciferase activities are the average of three experiments and are normalized relative to a control reporter and to maximum activity levels.

have apparent K_Ds for Smo binding that are similar to their IC_{50}s in pathway inhibition, either in the Shh-LIGHT2 assay or in cells lacking Ptch1 function (Fig. 3 *B* and *C*; Table 1). These compounds also counteract SAG-induced pathway activation in Shh-LIGHT2 cells (Fig. 3*D*). SANT-1, however, exhibits an apparent affinity for Smo that is 17-fold higher than would be expected from its inhibitory activity in these cell-based assays. SANT-1 also attenuates SAG stimulation of Shh-LIGHT2 cells

to a much greater extent than the other antagonists, inhibiting SAG activity by 60-fold as compared with 10-fold (Fig. 3*D*; Table 1) at similar inhibitory equivalents (5-fold greater than their IC_{50}s in the Shh-LIGHT2 assay).

Further distinctions between cyclopamine and the other Smo antagonists are revealed by their differential actions in the BODIPY-cyclopamine/Smo binding assay and on SmoA1 activity. In these experiments, the Smo-expressing cells were fixed with paraformaldehyde before the binding assay, thereby eliminating contributions from endocytosis and other trafficking processes. Although all four SANT compounds are able to block BODIPY-cyclopamine binding to Smo-expressing cells, SANT-1 and SANT-3 are unable to inhibit completely this association to background levels (Fig. 3*C*). In addition, the four SANT compounds block pathway activation in SmoA1-LIGHT2 cells with potencies similar to those observed in the Shh-LIGHT2 assay (Fig. 3 *B* and *E*; Table 1), whereas the SmoA1 mutation attenuates KAAD-cyclopamine activity by 15-fold (24). SANT-3 is also unique in that it can fully suppress Shh signaling in Shh-LIGHT2 cells (see Fig. 3*B*), but can only partially suppress constitutive pathway activity in SmoA1-LIGHT2 cells (Fig. 3*E*). Thus, although cyclopamine, SANT-1, -2, -3, and -4 all inhibit Hh pathway activity and block BODIPY-cyclopamine binding to Smo, their specific mechanisms appear to vary.

Discussion

Smo Activity Can Be Modulated by Small Molecules. Among Hh pathway components, Smo appears to be particularly susceptible to small molecule perturbation. Previous studies have demonstrated that cyclopamine inhibits Hh signaling by binding directly to Smo (25), and our investigations now reveal that Smo is also targeted by SAG, an Hh pathway agonist. Furthermore, an unbiased screen for additional pathway modulators yielded six inhibitors, including four specific Smo antagonists (SANT-1 through SANT-4). In general, the inhibitory activities of cyclopamine and the SANT compounds in the Shh-LIGHT2 assay closely match their apparent affinities for Smo, as determined by the BODIPY-cyclopamine binding competitions. These results are consistent with a loss-of-function mechanism, in which ligand binding inhibits Smo activity. The apparent K_D of the SAG/Smo complex (59 nM), in contrast, is significantly higher than the SAG EC_{50} for pathway activation (3 nM). This difference may reflect a gain-of-function mechanism, if only a fraction of Smo in its active state is required for maximum pathway activation. Alternatively, SAG binding to endogenous Smo in Shh-LIGHT2 cells may be promoted by cellular factors that do not significantly participate in the binding of SAG to overexpressed Smo in Cos-1 cells (see below; Fig. 4).

The ability of Smo to respond in distinct ways to different ligands raises important questions about the mechanisms of Smo function and small molecule action. Smo shares some structural homology with the G protein coupled receptor family, which

Table 1. Inhibition of *SAG* activity

Compound	Shh-LIGHT2*, nM	SmoA1-LIGHT2[†], nM	Ptch1[−/−‡], nM	SAG inhibition[§]	K_D[¶], nM	PA-cyc competition[‖]
SANT-1	20	30	20	60-fold	1.2	+
SANT-2	30	70	50	10-fold	12	+
SANT-3	100	80	80	10-fold	44	+
SANT-4	200	300	300	10-fold	71	+

*IC_{50} in the Shh-LIGHT2 assay using ShhNp as described.
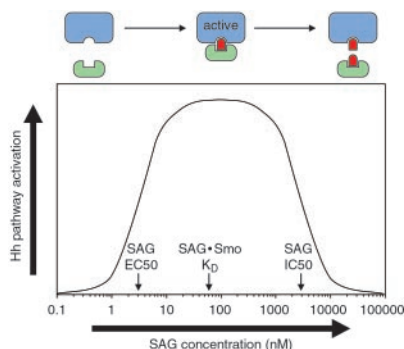[†]IC_{50} in the SmoA1-LIGHT2 assay as described.
[‡]IC_{50} in cells derived from Ptch1^{−/−} embryos, using β-galatosidase activity as a measure of pathway activation.
[§]Attenuation of SAG activity in Shh-LIGHT2 cells.
[¶]Apparent K_D determined by the BODIPY-cyclopamine binding competition assay.
[‖]Ability to compete the crosslinking of Smo-Myc$_3$ by PA-cyclopamine.

Fig. 4. A bivalent model of SAG action. Hh pathway stimulation or inhibition by SAG at low or high concentrations, respectively, can be accounted for by bivalent binding of SAG to Smo and to a downstream effector. In this model, Hh pathway activation would normally involve the recruitment of a downstream effector (green) by a subpopulation of Smo molecules (blue). At subsaturating concentrations, SAG (red) can bind both Smo and the effector, thereby promoting Smo/effector association and increasing pathway activity levels. Higher concentrations of SAG, however, can inhibit the formation of this ternary complex by independently binding both proteins.

utilizes a global conformational change in protein structure to link the binding of extracellular ligands to the recruitment of intracellular G proteins (31). A physiological role for G proteins in Hh signaling has not been found, but the differing activities of cyclopamine, SAG, and the SANT compounds suggest that a similar conformational change is the primary determinant of Smo activity. We have shown, for example, that cyclopamine and SAG specifically target the Smo heptahelical bundle (see above) and that both compounds facilitate the movement of SmoA1 through the ER quality control system, presumably by affecting its protein structure (25).

SANTs May Differ Mechanistically. In principle, cyclopamine, SAG, and the SANT compounds might interact with a common set of Smo residues or occupy allosteric sites. Although it is difficult to distinguish between these two possibilities without a comprehensive analysis of small molecule interactions with purified Smo protein, our current results provide evidence that the Smo antagonists may act by different mechanisms. The inability of SANT-1 and SANT-3 to inhibit completely the association of BODIPY-cyclopamine to Smo-expressing cells suggests that their interactions with Smo may alter its affinity for cyclopamine rather than compete directly for cyclopamine binding. SANT-1 and SANT-3 also appear to differ mechanistically from each other, as only SANT-1 can inhibit pathway activation induced by SmoA1 overexpression to background levels. These observations suggest that Smo can adopt multiple protein conformations with varying degrees of activity.

The small molecule antagonists may even interact with Smo in chemically distinct ways. Unlike cyclopamine and the other SANT compounds, SANT-1 has disparate inhibitory activities in the Shh-LIGHT2 and BODIPY-cyclopamine assays and is unusually potent at blocking SAG-mediated pathway activation. These properties may be caused by the hydrazone linkage in SANT-1, which is susceptible to hydrolysis and could form a covalent adduct with Smo upon binding. Such a SANT-1/Smo conjugate would be highly resistant to SAG, and accordingly, chemical reduction of the hydrazone moiety produces a compound with significantly diminished activity (J.K.C. and P.A.B., unpublished data).

Smo Activity May Be Regulated by Endogenous Small Molecules. The mechanisms by which endogenous cellular components regulate Smo activity remain elusive, although recent studies suggest that

Ptc acts catalytically through an indirect mechanism (19–21, 32). In comparison, the molecular basis for activation of the Frizzled family of seven-transmembrane receptors, which are closely related to Smo in structure, is well characterized. The Frizzled proteins form coreceptors with a low-density lipoprotein receptor-related protein (33, 34), and their activation is contingent on the binding of Wnt ligands to their extracellular cysteine-rich domains (CRDs; ref. 35). No analogous protein partners have been associated with Smo activation, and the Smo CRD does not appear to be required for its activity or regulation by Ptc (21).

Within this context, the susceptibility of Smo to chemical modulation and the structural similarities between Ptc, the RND permeases, and NPC1 suggest that Smo regulation may involve physiological small molecules rather than direct protein–protein interactions. One possibility is that Ptc regulates the subcellular and/or intramembrane distribution of an endogenous small molecule, thereby influencing Smo activity. This regulatory effect could be caused by Ptc-dependent changes in Smo localization, because asymmetric distributions of membrane components can affect vesicle formation and trafficking (36). The subcellular localization of Smo then might be associated with specific Smo activity states, as each cellular compartment has unique membrane compositions (36), and Smo might respond differentially to distinct molecular environments. Alternatively, Ptc might directly modulate the localization of an endogenous Smo ligand. This putative Ptc substrate could either be a Smo agonist or antagonist, depending on how Ptc function influences this molecule's activity.

The suppression of maximum levels of SAG-mediated pathway activation by Ptch1 expression (see Fig. 1*H*) provides some constraints to these models. Furthermore, we have previously found that higher Ptch1 expression levels coincide with an increase in cyclopamine binding to Smo (25). These results suggest that Ptch1 might promote interactions between Smo and a physiological inhibitor that facilitates cyclopamine binding but also effectively inhibits the SAG/Smo complex. A more likely scenario, perhaps, is that Ptch1 acts to redistribute Smo to subcellular compartments that are nonpermissive for SAG binding because of concomitant changes in Smo conformation and/or the unavailability of effector proteins (see below). The inactive Smo protein in such signaling-incompetent compartments might, therefore, preferentially bind cyclopamine.

SAG Activity Provides Evidence for a Downstream Effector. One interesting aspect of SAG activity is its diminished potency at concentrations above 1 μM (see Fig. 2*B*). This loss of pathway activity is not caused by cytotoxicity, as indicated by measurements of control reporter constructs (not shown), which suggests that SAG not only binds to Smo but can also inhibit a cellular component required for Hh signaling. The SAG-mediated reduction in pathway activity appears to involve a target other than Smo, as neither KAAD-cyclopamine nor SANT-2, -3, or -4 affect the inhibitory activity of higher SAG concentrations, despite their dramatic effects on the stimulatory activity of lower SAG concentrations (see Figs. 1*F* and 3*D*). A possible explanation for this behavior is that SAG may interact not only with Smo, but also with a cellular effector of Smo activation, thereby inducing Hh pathway activation by facilitating the association of these two proteins at optimal SAG concentrations (Fig. 4). Higher SAG concentrations, however, would begin to inhibit this process, as the agonist would independently bind both Smo and effector.

The cooperative interactions within this putative ternary complex might also explain the restriction of PA-SAG cross-linking to post-ER Smo, as the association of Smo with its downstream effector probably occurs outside the ER, and additional protein contacts might be required to compensate for the reduced activity of PA-SAG. Similarly, the resistance of the PA-SAG/Smo cross-linking reaction to KAAD-cyclopamine competition

BIOCHEMISTRY

could reflect differential interactions between the small molecules and the Smo/effector complex in comparison to Smo protein alone. The functional and biochemical activities of SAG are also consistent with a ternary complex model, because the apparent K_D for the SAG/Smo complex (59 nM) is significantly greater than the SAG EC$_{50}$ in Shh-LIGHT2 cells (3 nM). If SAG indeed has bivalent activity, its ability to inhibit pathway activation with an IC$_{50}$ of 3 μM suggests that the putative agonist-effector complex has a K_D in the low micromolar range.

Mechanistic Differences Between the SANTs May Be Therapeutically Useful. Our identification of Smo as the target of SAG and four synthetic antagonists underscores its susceptibility to small molecule modulation and raises the possibility that endogenous small molecules similarly regulate Smo activity. These studies also may provide additional reagents for the pharmacological manipulation of Hh pathway activity, as inappropriate pathway activation is associated with oncogenesis. Many Hh-related tumors involve a loss of Ptch1 function (2–4), and the structural mutation in SmoA1 was discovered as a somatic lesion in basal cell carcinoma (37), indicating the therapeutic potential of Smo antagonists. Accordingly, recent studies demonstrate the ability of cyclopamine to prevent the growth of Ptch1-deficient medulloblastoma in mice (29).

Tumors associated with oncogenic mutations in Smo, however, may be less responsive to cyclopamine treatment, as indicated by the resistance of SmoA1 to cyclopamine-mediated inhibition. In these cases, the SANT compounds and analogs thereof may prove to be therapeutically preferable to cyclopamine. Unlike cyclopamine and its derivatives, the SANT compounds are nearly equipotent against the activities of WT and oncogenic Smo, with SANT-1 and SANT-2 as particularly potent inhibitors of SmoA1. These results further indicate that the SANT compounds and cyclopamine may inhibit Smo activity by different biochemical mechanisms and represent a promising step toward pathway-specific cancer treatments.

Note Added in Proof. Similar results demonstrating the action of SAG on Smo are reported in ref. 38.

1. Ingham, P. W. & McMahon, A. P. (2001) *Genes Dev.* **15,** 3059–3087.
2. Goodrich, L. V. & Scott, M. P. (1998) *Neuron* **21,** 1243–1257.
3. Taipale, J. & Beachy, P. A. (2001) *Nature* **411,** 349–354.
4. Wicking, C. & McGlinn, E. (2001) *Cancer Lett.* **173,** 1–7.
5. Hooper, J. E. & Scott, M. P. (1989) *Cell* **59,** 751–765.
6. Nakano, Y., Guerrero, I., Hidalgo, A., Taylor, A., Whittle, J. R. & Ingham, P. W. (1989) *Nature* **341,** 508–513.
7. Alcedo, J., Ayzenzon, M., Von Ohlen, T., Noll, M. & Hooper, J. E. (1996) *Cell* **86,** 221–232.
8. Stone, D. M., Hynes, M., Armanini, M., Swanson, T. A., Gu, Q., Johnson, R. L., Scott, M. P., Pennica, D., Goddard, A., Phillips, H., *et al*. (1996) *Nature* **384,** 129–134.
9. van den Heuvel, M. & Ingham, P. W. (1996) *Nature* **382,** 547–551.
10. Marigo, V., Davey, R. A., Zuo, Y., Cunningham, J. M. & Tabin, C. J. (1996) *Nature* **384,** 176–179.
11. Fuse, N., Maiti, T., Wang, B., Porter, J. A., Hall, T. M., Leahy, D. J. & Beachy, P. A. (1999) *Proc. Natl. Acad. Sci. USA* **96,** 10992–10999.
12. Kalderon, D. (2000) *Cell* **103,** 371–374.
13. Aza-Blanc, P., Ramirez-Weber, F. A., Laget, M. P., Schwartz, C. & Kornberg, T. B. (1997) *Cell* **89,** 1043–1053.
14. Chen, C. H., von Kessler, D. P., Park, W., Wang, B., Ma, Y. & Beachy, P. A. (1999) *Cell* **98,** 305–316.
15. Nusslein-Volhard, C., Wieschaus, E. & Kluding, H. (1984) *Roux's Arch. Dev. Biol.* **193,** 267–282.
16. Zhang, X. M., Ramalho-Santos, M. & McMahon, A. P. (2001) *Cell* **106,** 781–792.
17. Barresi, M. J., Stickney, H. L. & Devoto, S. H. (2000) *Development (Cambridge, U.K.)* **127,** 2189–2199.
18. Chen, W., Burgess, S. & Hopkins, N. (2001) *Development (Cambridge, U.K.)* **128,** 2385–2396.
19. Denef, N., Neubuser, D., Perez, L. & Cohen, S. M. (2000) *Cell* **102,** 521–531.
20. Ingham, P. W., Nystedt, S., Nakano, Y., Brown, W., Stark, D., van den Heuvel, M. & Taylor, A. M. (2000) *Curr. Biol.* **10,** 1315–1318.
21. Taipale, J., Cooper, M. K., Maiti, T. & Beachy, P. A. (2002) *Nature* **418,** 892–896.
22. Cooper, M. K., Porter, J. A., Young, K. E. & Beachy, P. A. (1998) *Science* **280,** 1603–1607.
23. Incardona, J. P., Gaffield, W., Kapur, R. P. & Roelink, H. (1998) *Development (Cambridge, U.K.)* **125,** 3553–3562.
24. Taipale, J., Chen, J. K., Cooper, M. K., Wang, B., Mann, R. K., Milenkovic, L., Scott, M. P. & Beachy, P. A. (2000) *Nature* **406,** 1005–1009.
25. Chen, J. K., Taipale, J., Cooper, M. K. & Beachy, P. A. (2002) *Genes Dev.*, in press.
26. Tseng, T. T., Gratwick, K. S., Kollman, J., Park, D., Nies, D. H., Goffeau, A. & Saier, M. H., Jr. (1999) *J. Mol. Microbiol. Biotechnol.* **1,** 107–125.
27. Davies, J. P., Chen, F. W. & Ioannou, Y. A. (2000) *Science* **290,** 2295–2298.
28. Baxter, A. D., Boyd, E. A., Guicherit, O. M., Porter, J., Price, S. & Rubin, L. E. (2001) PCT Int. Appl., WO 2001-US10296.
29. Berman, D. M., Karhadkar, S. S., Hallahan, A. R., Pritchard, J. I., Eberhart, C. G., Watkins, N., Chen, J. K., Cooper, M. K., Taipale, J., Olson, J. M. & Beachy, P. A. (2002) *Science* **297,** 1559–1561.
30. Goodrich, L. V., Milenkovic, L., Higgins, K. M. & Scott, M. P. (1997) *Science* **277,** 1109–1113.
31. Christopoulos, A. & Kenakin, T. (2002) *Pharmacol. Rev.* **54,** 323–374.
32. Incardona, J. P., Gruenberg, J. & Roelink, H. (2002) *Curr. Biol.* **12,** 983–995.
33. Pinson, K. I., Brennan, J., Monkley, S., Avery, B. J. & Skarnes, W. C. (2000) *Nature* **407,** 535–538.
34. Wehrli, M., Dougan, S. T., Caldwell, K., O'Keefe, L., Schwartz, S., Vaizel-Ohayon, D., Schejter, E., Tomlinson, A. & DiNardo, S. (2000) *Nature* **407,** 527–530.
35. Bhanot, P., Brink, M., Samos, C. H., Hsieh, J. C., Wang, Y., Macke, J. P., Andrew, D., Nathans, J. & Nusse, R. (1996) *Nature* **382,** 225–230.
36. Sprong, H., van der Sluijs, P. & van Meer, G. (2001) *Nat. Rev. Mol. Cell. Biol.* **2,** 504–513.
37. Lam, C. W., Xie, J., To, K. F., Ng, H. K., Lee, K. C., Yuen, N. W., Lim, P. L., Chan, L. Y., Tong, S. F. & McCormick, F. (1999) *Oncogene* **18,** 833–836.
38. Frank-Kamenetsky, M., Zhang, X. M., Bottega, S., Guicherit, O., Wichterle, H., Dudek, D., Bumcrot, D., Wang, F., Jones, S., Shulok, J., Rubin, L. & Porter, J. A. (2002) *J. Biol.*, in press.